2014

KAP-1 promotes resection of broken DNA ends not protected by γ-H2AX and 53BP1 in G1-phase lymphocytes

Anthony T. Tubbs
Washington University School of Medicine in St. Louis

Yair Dorsett
Washington University School of Medicine in St. Louis

Elizabeth Chan
Duke University

Beth Helmink
Washington University School of Medicine in St. Louis

Baeck-Seung Lee
Washington University School of Medicine in St. Louis

See next page for additional authors

Molecular and Cellular Biology

KAP-1 Promotes Resection of Broken DNA Ends Not Protected by γ-H2AX and 53BP1 in G $_1$-Phase Lymphocytes

Anthony T. Tubbs, Yair Dorsett, Elizabeth Chan, Beth Helmink, Baeck-Seung Lee, Putzer Hung, Rosmy George, Andrea L. Bredemeyer, Anuradha Mittal, Rohit V. Pappu, Dipanjan Chowdhury, Nima Mosammaparast, Michael S. Krangel and Barry P. Sleckman

Mol. Cell. Biol. **2014, 34(15):2811. DOI: 10.1128/MCB.00441-14.**
Published Ahead of Print 19 May 2014.

MCB
Journals.ASM.org

KAP-1 Promotes Resection of Broken DNA Ends Not Protected by γ-H2AX and 53BP1 in G_1-Phase Lymphocytes

Anthony T. Tubbs,[a] Yair Dorsett,[a] Elizabeth Chan,[b] Beth Helmink,[a] Baeck-Seung Lee,[a] Putzer Hung,[a] Rosmy George,[a] Andrea L. Bredemeyer,[a] Anuradha Mittal,[c] Rohit V. Pappu,[c] Dipanjan Chowdhury,[d] Nima Mosammaparast,[a] Michael S. Krangel,[b] Barry P. Sleckman[a]

Department of Pathology and Immunology, Washington University School of Medicine, St. Louis, Missouri, USA[a]; Department of Immunology, Duke University Medical Center, Durham, North Carolina, USA[b]; Department of Biomedical Engineering and Center for Biological Systems Engineering, Washington University, St. Louis, Missouri, USA[c]; Department of Radiation Oncology, Harvard Medical School, Boston, Massachusetts, USA[d]

The resection of broken DNA ends is required for DNA double-strand break (DSB) repair by homologous recombination (HR) but can inhibit normal repair by nonhomologous end joining (NHEJ), the main DSB repair pathway in G_1-phase cells. Antigen receptor gene assembly proceeds through DNA DSB intermediates generated in G_1-phase lymphocytes by the RAG endonuclease. These DSBs activate ATM, which phosphorylates H2AX, forming γ-H2AX in flanking chromatin. γ-H2AX prevents CtIP from initiating resection of RAG DSBs. Whether there are additional proteins required to promote resection of these DNA ends is not known. KRAB-associated protein 1 (KAP-1) (TRIM28) is a transcriptional repressor that modulates chromatin structure and has been implicated in the repair of DNA DSBs in heterochromatin. Here, we show that in murine G_1-phase lymphocytes, KAP-1 promotes resection of DSBs that are not protected by H2AX and its downstream effector 53BP1. In these murine cells, KAP-1 activity in DNA end resection is attenuated by a single-amino-acid change that reflects a KAP-1 polymorphism between primates and other mammalian species. These findings establish KAP-1 as a component of the machinery that can resect DNA ends in G_1-phase cells and suggest that there may be species-specific features to this activity.

The repair of DNA double-strand breaks (DSBs) is carried out by either homologous recombination (HR) or nonhomologous end joining (NHEJ) (1, 2). HR functions to repair DSBs generated in the S and G_2 phases of the cell cycle. In contrast, NHEJ functions to repair DSBs at all phases of the cell cycle, and in G_1-phase cells, it is the primary DSB repair pathway. DNA end resection and the formation of single-strand overhangs are critical steps in repair pathway choice (3, 4). During HR, CtIP promotes the processing of DNA ends, forming 3′ single-strand overhangs that bind RPA, initiating HR (3, 4). In contrast, NHEJ most efficiently repairs DNA ends that are blunt or that have short single-strand overhangs (4).

Lymphocyte antigen receptor gene assembly occurs through the process of V(D)J recombination (5). This reaction is initiated by RAG-1 and RAG-2, which form the RAG endonuclease (6). RAG introduces DNA DSBs at the border of two recombining gene segments, forming a hairpin-sealed coding end and a blunt signal end at each DSB (6). NHEJ joins the coding ends, forming a coding joint, and the signal ends, forming a signal joint (7, 8). The NHEJ proteins required for V(D)J recombination include Ku70, Ku80, and the catalytic subunit of DNA-dependent protein kinase (DNA-PKcs), which together form the DNA-PK complex (7, 8). The Artemis endonuclease is required to open hairpin-sealed coding ends, and DNA ligase IV ligates the signal and coding ends (7, 8). XRCC4 functions with DNA ligase IV to promote joining (7, 8). XLF also functions in the repair of RAG DSBs, but this function is redundant with other factors (9–11). V(D)J recombination occurs only in the G_1 phase of the cell cycle, due in part to the degradation of RAG-2 during S phase (12).

RAG DSBs activate the ATM kinase and DNA damage responses (DDRs) (7). This includes the phosphorylation of the histone variant H2AX (forming γ-H2AX) in chromatin for several hundred kilobases flanking RAG DSBs (13). In G_1-phase cells, the formation of γ-H2AX prevents CtIP from initiating the resection of RAG DSBs (11). Indeed, in H2AX-deficient lymphocytes, CtIP promotes hairpin opening and resection of coding ends in the absence of Artemis (11). Whether additional proteins also function in this resection process is not known.

KRAB-associated protein 1 (KAP-1) (also known as TRIM28, TIF1β, or KRIP-1) has been implicated in DNA DSB repair (14–16). KAP-1 is a member of the tripartite motif (TRIM) family of proteins, which includes approximately 100 members in humans (17–20). These proteins have N-terminal tripartite motifs composed of RING, B-box, and coiled-coil domains that promote homo- and hetero-oligomerization (17–19). This oligomerization is important for the stability and function of many TRIM proteins. The C termini of the TRIM proteins are diverse and composed of domains that mediate the many different functions of these proteins, including transcriptional regulation, modulation of signaling pathways, alteration of chromatin structure, pathogen recognition, and DNA DSB repair. TRIM proteins can exhibit significant polymorphisms over short evolutionary distances that may be important for some of their species-specific functions, such as pathogen recognition and defense (18–20).

KAP-1 is involved in the repair of DSBs generated in heterochromatic regions of the genome in both mouse and human cells (15, 21). KAP-1 has a C-terminal plant homeodomain (PHD)

Received 1 April 2014 Returned for modification 1 May 2014
Accepted 12 May 2014
Published ahead of print 19 May 2014
Address correspondence to Barry P. Sleckman, sleckman@immunology.wustl.edu.

doi:10.1128/MCB.00441-14

with E3 SUMO ligase activity, required for binding of the nucleosome remodeler CHD3 to the adjacent bromodomain (22). The C terminus of KAP-1 also contains a serine residue (serine 824) that is phosphorylated by ATM in response to DNA DSBs (14). Phosphorylation of this residue disrupts the interaction of KAP-1 and CHD3, which is required for efficient repair of heterochromatic DSBs (21–23). The DNA repair factor 53BP1, which localizes to chromatin containing γ-H2AX, is required for optimal heterochromatic DSB repair mediated by KAP-1 phosphorylation and chromatin relaxation (23, 24). 53BP1 has also been implicated in preventing DNA end resection, antagonizing HR and promoting NHEJ (24–28).

Here, we show that mouse KAP-1 (mKAP-1) functions to promote the resection of DNA DSBs in murine G_1-phase lymphocytes when these DNA ends are not protected by H2AX and 53BP1. A single-amino-acid change that reflects a KAP-1 polymorphism between primates and other mammalian species disrupts its ability to promote DNA end resection in murine cells. These findings establish a novel function for KAP-1 in DNA DSB repair. The potential species-specific aspects of this KAP-1 function are discussed.

MATERIALS AND METHODS

Cell culture. Abelson-transformed pre-B cells that express a Bcl2 transgene (abl pre-B cells) were generated, and the pMX-DEL^{CJ} retroviral recombination substrate was introduced as previously described (29). The generation of *LigIV*$^{-/-}$ abl pre-B cells from *LigIV*$^{LoxP/LoxP}$ abl pre-B cells was carried out as previously described (11). For RAG induction, abl pre-B cells were treated with 3 μM imatinib for the indicated number of days at 10^6 cells/ml. The ATM kinase inhibitor KU55933 (Tocris) was used at 15 μM.

Southern blotting. Native and denaturing (1.2% agarose and 1 M urea) Southern blot analyses of V(D)J recombination of the pMX-DEL^{CJ} retroviral recombination substrate were carried out as previously described (11). Southern blot analyses of Eb:ZFN (zinc finger nuclease) DSBs were performed as previously described (30). The Eb probe was generated by PCR amplification using the oligonucleotides 5′-GTTAAC CAGGCACAGTAGGAC-3′ and 5′-CCATGGTGCATACTGAAGGC-3′. The Erag probe was generated by PCR amplification using the oligonucleotides 5′-AACTTCCTCCAGCAGGCGATCT-3′ and 5′-TTGACTGT CAGTTCAGCCAAA-3′.

Immunofluorescence. abl pre-B cells were treated with imatinib for 2 days. A total of 10^6 cells were washed in 1× phosphate-buffered saline (PBS) and attached to glass slides coated with Cell-Tak (BD). Cells were fixed with 4% formaldehyde in PBS for 10 min at room temperature, permeabilized in 0.5% Triton X-100 in PBS for 5 min, and then washed with PBS. Coimmunostaining with primary and secondary antibodies was performed with a blocking solution of 3% bovine serum albumin (BSA) in PBS at 37°C for 1 h, and cells were mounted with ProLong Gold Antifade reagent containing 4′,6-diamidino-2-phenylindole (DAPI) (Invitrogen). Antibodies used for staining were anti-γ-H2AX clone JBW301 (1:2,000 dilution) (Millipore), anti-53BP1 (1:500) (H-300; Santa Cruz), Alexa Fluor 488–goat anti-rabbit IgG (1:2,000), and Alexa Fluor 594–goat anti-mouse IgG (1:2,000). Imaging was performed with a microscope (BX-53; Olympus), using an ApoN 60×/1.49-numerical-aperture (NA) oil immersion lens and cellSens Dimension software. For each experiment, >50 nuclei were observed from at least two individual cell lines. Immunofluorescent *in situ* hybridization (immuno-FISH), confocal imaging, and colocalization analysis were performed as previously described (31). *Igk* was visualized by using a bacterial artificial chromosome (BAC) for 3′ Cκ (RP23-341D5). 53BP1 was visualized by using an anti-53BP1 antibody (NB 100-304; Novus Biologicals) and fluorescein isothiocyanate (FITC)-conjugated donkey anti-rabbit IgG (sc-2090; Santa Cruz Biotechnology). Images were collected on a Leica SP5 confocal microscope with optical sections separated by 0.12 μm. Three-dimensional distances between the centers of mass of two foci were measured by using the Sync Measure 3D ImageJ plug-in. *Igk* alleles were scored as 53BP1 positive (53BP1$^+$) when the center-to-center distance between the *Igk* and 53BP1 foci was 1 μm or less.

Lentiviral knockdown and retroviral cDNA expression. Knockdown using lentiviral U6 short hairpin RNAs (shRNAs) was performed with a pFLRU:Thy1.1 lentiviral vector derived from pFLRU:YFP, which was described previously (11). We replaced the yellow fluorescent protein (YFP) cDNA in the original vector with Thy1.1 cDNA and then cloned it into U6 shRNAs to generate pFLRU:shRNA:Thy1.1 vectors. The shRNA sense sequences used were 5′-GGGATATGGCTTTGGGTCA-3′ for KAP-1, 5′-G AGCAGACCTTTCTCAGTA-3′ for CtIP, and 5′-GGTTCGATGTCCCA ATTCTG-3′ as a nontargeting control (ctr). Lentiviruses were generated and abl pre-B cells were transduced as previously described (11). Cells expressing the pFLRU-shRNA vectors were obtained by magnetic cell sorting using CD90.1 (Thy1.1) MicroBeads and MS columns (Miltenyi).

Plasmids for expression of human KAP-1 (hKAP-1) cDNAs were derived from pOZ-FH-N-KAP1 (32). The mouse KAP-1 cDNA was generating by using RNA from a wild-type C57BL/6J mouse. Mouse KAP-1 was cloned downstream of the Flag-hemagglutinin (Flag-HA) tag in pOZ-FH-N by using XhoI/NotI, replacing the human KAP-1 cDNA. Flag-tagged KAP-1 hybrids were generated by PCR amplification of mouse or human cDNA. An shRNA-resistant mouse KAP-1 cDNA was generated by changing 3 nucleotides in the mouse KAP-1 cDNA complementary to the KAP-1 shRNA. Flag-tagged KAP-1 hybrids and point mutants were cloned into pOZ-FH-N. Retrovirus were generated and transduced into abl pre-B cells as previously described (11). Cells expressing the pOZ vectors were obtained by magnetic cell sorting using human CD25 MicroBeads and MS columns (Miltenyi).

Immunoblot analysis. Whole-cell lysates were generated by using LDS sample buffer (Invitrogen) supplemented with dithiothreitol (DTT). Standard immunoblotting techniques were used, as previously described (11). Primary antibodies used include anti-KAP-1 (rabbit polyclonal, recognizing mouse and human KAP-1; GeneTex), anti-Flag M2 (Sigma), and anti-glyceraldehyde-3-phosphate dehydrogenase (GAPDH) (Sigma).

Analysis of protein structure order. Protein disorder for mKAP-1 and hKAP-1 was predicted by PrDOS (http://prdos.hgc.jp/cgi-bin/top.cgi), using protein sequences for mKAP-1 (NCBI accession number NP_035718.2) and hKAP-1 (accession number NP_005753.1) (33). A 5% false-positive rate was used.

Induction of DSBs using zinc finger nucleases. A pair of custom zinc finger nucleases (Eb:ZFN), Eb1:ZFN and Eb2:ZFN, specific to a region of the mouse T cell receptor beta (*Tcrb*) locus near the enhancer (*Eb*), were previously described (30). Eb1:ZFN and Eb2:ZFN were expressed under a tetracycline-responsive element with a constitutively expressed Thy1.1 or Thy1.2 marker, generating the lentiviral vectors TRE-Eb1:ZFN-Thy1.2 and TRE-Eb2:ZFN-Thy1.1. The lentivirus was generated and abl pre-B cells were transduced as previously described (11). Cells expressing both Thy1.1 and Thy1.2 were selected by magnetically activated cell sorting (MACS) (Miltenyi) in consecutive sorts for individual markers. Cells with Eb:ZFN were treated with imatinib for 1 day to arrest cells in G_1 phase and 4 μg/ml doxycycline (Sigma) for either 1 or 2 days.

RPA-binding assay. The RPA-binding assay was performed as previously described, with the following modifications (34). abl pre-B cells treated with imatinib for 2 days were subjected to 5 μg/ml bleocin treatment for 24 h before preextraction with 0.2% Triton X-100. Fixation and permeabilization were performed with Fix/Perm solution (BD Biosciences). RPA32 staining was performed with Perm Wash (BD Biosciences) with anti-RPA32 antibody (rat monoclonal antibody [MAb], clone 4E4; Cell Signaling) (1:1,000 dilution). Secondary staining was performed by using Alexa Fluor 488–goat anti-rat IgG (Invitrogen). DNA content was assayed by using 7-aminoactinomycin D (7AAD), and stained cells were analyzed by using a FACSCalibur instrument.

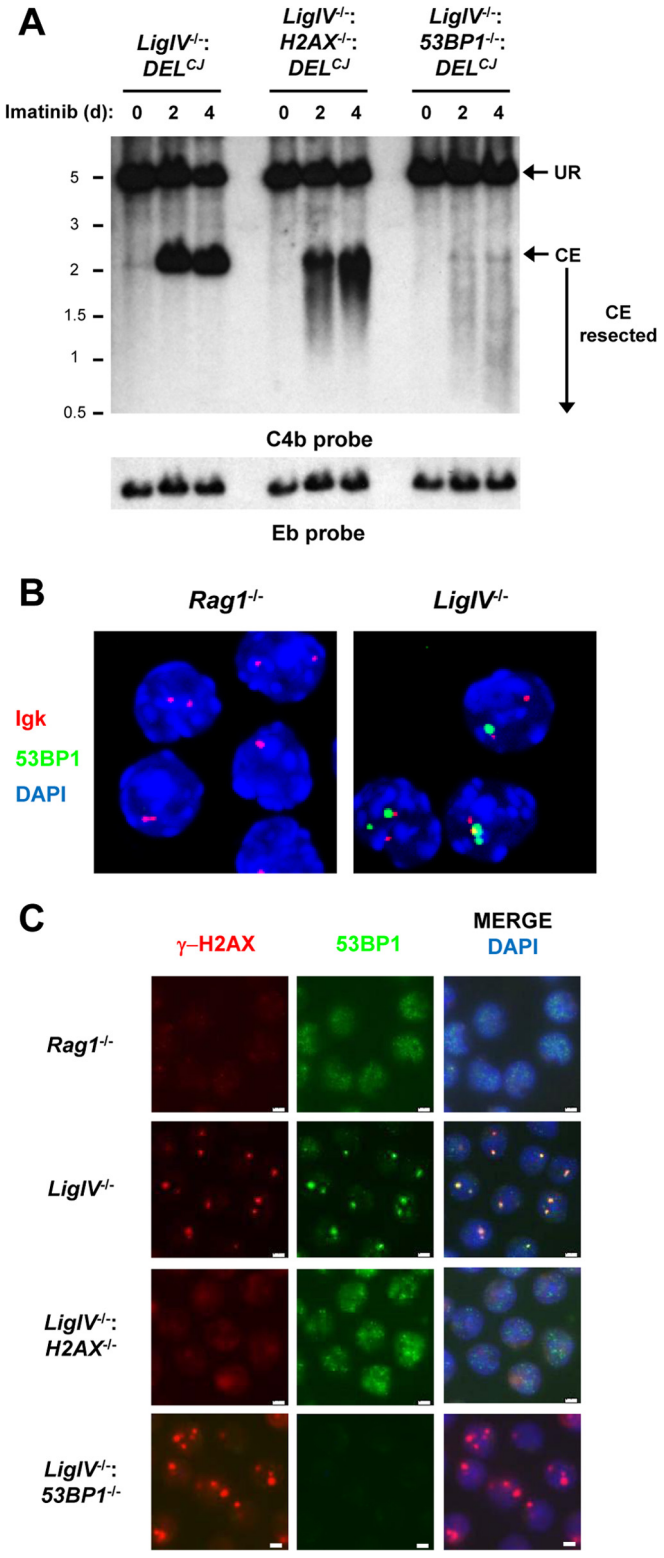

FIG 1 53BP1 inhibits resection of RAG DSBs. (A) Southern blot analysis of pMX-DEL^{CJ} in abl pre-B cells treated with imatinib for 0, 2, or 4 days. Genomic DNA was digested with EcoRV and hybridized with the C4b probe. The bands generated by unrearranged pMX-DEL^{CJ} (UR) and full-length (2.2-kb) pMX-DEL^{CJ} coding ends (CE) are indicated. Resected coding ends have a lower molecular weight and are also indicated. Molecular size markers, in kilobases, are indicated. The Eb probe was used a DNA loading control. Data shown were generated from *LigIV*$^{-/-}$:*DEL*^{CJ}-7, *LigIV*$^{-/-}$:*H2AX*$^{-/-}$:*DEL*^{CJ}-5, and *LigIV*$^{-/-}$:*53BP1*$^{-/-}$:*DEL*^{CJ}-58 abl pre-B cells. Similar results were obtained for *LigIV*$^{-/-}$:*DEL*^{CJ}-1, *LigIV*$^{-/-}$:*H2AX*$^{-/-}$:*DEL*^{CJ}-148, and *LigIV*$^{-/-}$:*53BP1*$^{-/-}$:*DEL*^{CJ}-5 abl pre-B cells. (B) Confocal immuno-FISH of *Rag1*$^{-/-}$ and *LigIV*$^{-/-}$ abl pre-B cells treated with imatinib for 2 days. Nuclei were probed by using a BAC for *Igk* (red) and were stained by using an anti-53BP1 antibody (green) and DAPI (blue). Composite three-dimensional images are displayed as z-projections. Data shown were generated from *Rag1*$^{-/-}$ (R1K) and *LigIV*$^{-/-}$ (ALig4) abl pre-B cells, and similar results were obtained for *Rag2*$^{-/-}$ (R2K2) and *LigIV*$^{-/-}$ (BLig4) abl pre-B cells. (C) Immunofluorescence assay for 53BP1 and γ-H2AX in abl pre-B cells treated with imatinib for 2 days. Bar, 1 μm. Data shown were generated from *Rag1*$^{-/-}$ (R1K), *LigIV*$^{-/-}$ (ALig4), *LigIV*$^{-/-}$:*H2AX*$^{-/-}$ (LH5), and *LigIV*$^{-/-}$:*53BP1*$^{-/-}$ (AL5) abl pre-B cells. Similar results were obtained for *LigIV*$^{-/-}$ (BLig4), *LigIV*$^{-/-}$:*H2AX*$^{-/-}$ (LH8), and *LigIV*$^{-/-}$:*53BP1*$^{-/-}$ (BL5) abl pre-B cells.

RESULTS

53BP1 inhibits resection of RAG DSBs in G_1-phase lymphocytes. The cellular responses to RAG DSBs can be assessed in Abelson-transformed pre-B cells that express a Bcl2 transgene, here referred to as abl pre-B cells (7, 29, 35). Treatment of these cells with the abl kinase inhibitor imatinib leads to G_1 cell cycle arrest, RAG induction, and initiation of V(D)J recombination at the endogenous immunoglobulin kappa (*Igk*) light chain locus and at chromosomally integrated retroviral recombination substrates, such as pMX-DEL^{CJ} (see the data posted at http://pathology.wustl.edu/labs/sleckman/Tubbs_et_a_MCB_2014_Supplement.pdf) (29). In abl pre-B cells with a single copy of pMX-DEL^{CJ} and deficient in Artemis (*Art*$^{-/-}$:*DEL*^{CJ}) or DNA ligase IV (*LigIV*$^{-/-}$:*DEL*^{CJ}), imatinib treatment leads to the accumulation of unrepaired coding ends at the *Igk* locus (see the data posted at the URL mentioned above) and pMX-DEL^{CJ} (Fig. 1A; see also the data posted at the URL mentioned above).

53BP1 foci form at RAG DSBs in *LigIV*$^{-/-}$ abl pre-B cells. This is evidenced by immuno-FISH analyses revealing that 66% (94/142) of 53BP1 foci colocalize with an *Igk* locus probe in *LigIV*$^{-/-}$ abl pre-B cells treated with imatinib (Fig. 1B). 53BP1 foci do not form in RAG-deficient (*Rag-1*$^{-/-}$) abl pre-B cells (Fig. 1C). Moreover, 53BP1 foci do not form at RAG DSBs in *LigIV*$^{-/-}$:*H2AX*$^{-/-}$ abl pre-B cells, in agreement with previous studies showing that 53BP1 retention at genotoxic DSBs depends on the formation of γ-H2AX (Fig. 1C) (24).

As has been observed for abl pre-B cells deficient in H2AX and either Artemis (*Art*$^{-/-}$:*H2AX*$^{-/-}$:*DEL*^{CJ}) or DNA ligase IV (*LigIV*$^{-/-}$:*H2AX*$^{-/-}$:*DEL*^{CJ}), pMX-DEL^{CJ} coding ends are also significantly resected in abl pre-B cells deficient in 53BP1 and either Artemis (*Art*$^{-/-}$:*53BP1*$^{-/-}$:*DEL*^{CJ}) or DNA ligase IV (*LigIV*$^{-/-}$:*53BP1*$^{-/-}$:*DEL*^{CJ}) (Fig. 1A; see also the data posted at http://pathology.wustl.edu/labs/sleckman/Tubbs_et_a_MCB_2014_Supplement.pdf) (11). Compared to H2AX-deficient cells, many of the pMX-DEL^{CJ} coding ends generated in 53BP1-deficient cells were undetectable, as they were resected past the C4b probe (Fig. 1A; see also the data posted at the URL mentioned above). Similar results were observed for coding ends generated at the *Igk* locus (data not shown). Thus, like H2AX, 53BP1 prevents resection of RAG DSBs in G_1-phase lymphocytes.

KAP-1 promotes resection of DNA breaks in G_1-phase cells. Because 53BP1 and KAP-1 are functionally connected in the repair of DSBs in heterochromatin, we hypothesized that CtIP-mediated resection in G_1-phase cells, which we have now linked to 53BP1, might also incorporate KAP-1 activity (23). We knocked down KAP-1 in *LigIV*$^{-/-}$:*H2AX*$^{-/-}$:*DEL*^{CJ} and *LigIV*$^{-/-}$:*53BP1*$^{-/-}$:*DEL*^{CJ} abl pre-B cells (Fig. 2A; see also the data posted at http://pathology.wustl.edu/labs/sleckman/Tubbs_et_a_MCB_2014_Supplement.pdf). Knock-

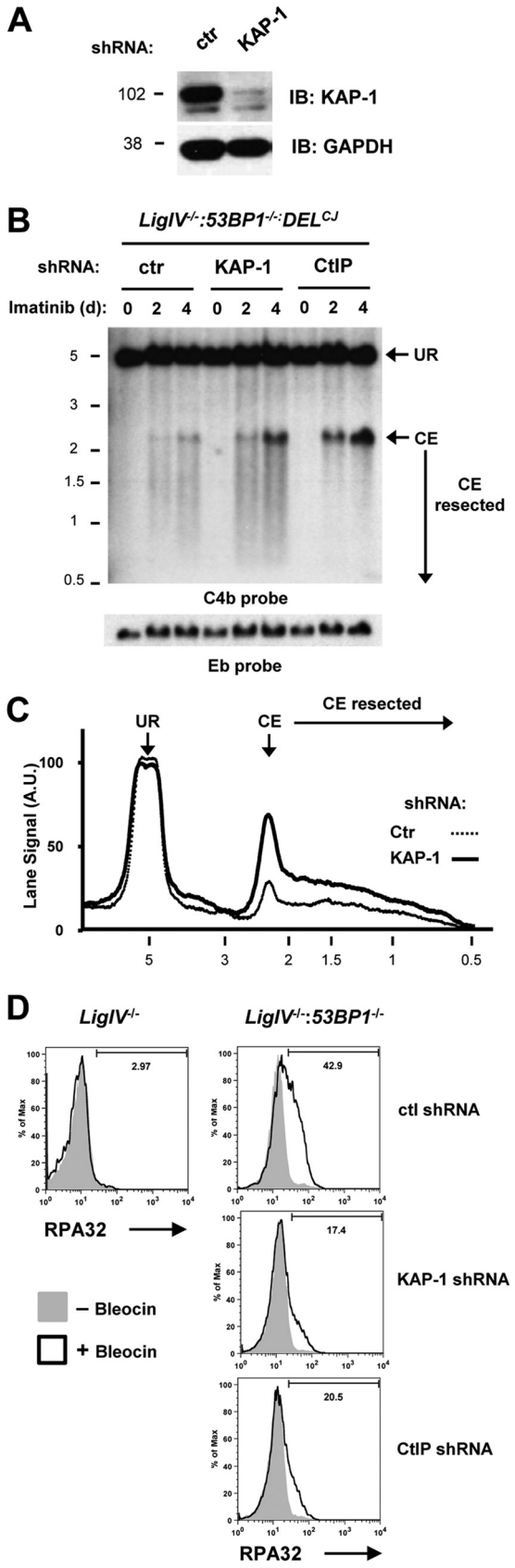

FIG 2 KAP-1 knockdown limits resection in G_1-phase lymphocytes. (A) Immunoblot (IB) analysis of KAP-1 expression in *LigIV*$^{-/-}$:*53BP1*$^{-/-}$ abl pre-B cells expressing either a KAP-1 or control (ctr) shRNA. GAPDH expression is shown as a protein loading control. Molecular mass markers, in kDa, are indicated. (B) Southern blot analysis of pMX-DEL^{CJ} as described in the legend of Fig. 1A. *LigIV*$^{-/-}$:*53BP1*$^{-/-}$:*DEL*^{CJ} abl pre-B cells expressing either ctr, KAP-1, or CtIP shRNA treated with imatinib for the indicated numbers of days were analyzed. Data shown were generated from *LigIV*$^{-/-}$:*53BP1*$^{-/-}$:*DEL*^{CJ}-6 abl pre-B cells, and similar results were obtained for *LigIV*$^{-/-}$:*53BP1*$^{-/-}$:*DEL*^{CJ}-58 abl pre-B cells. (C) Density plots comparing lane signals from *LigIV*$^{-/-}$:*53BP1*$^{-/-}$:*DEL*^{CJ} abl pre-B cells expressing either ctr or KAP-1 shRNA and treated with imatinib for 4 days, as shown in panel B. The signal was normalized for the Eb DNA loading control. Molecular size markers, in kilobases, are shown on the *x* axis. Peaks representing the unrearranged pMX-DEL^{CJ} (UR), full-length (2.2-kb) pMX-DEL^{CJ} coding ends (CE), and resected coding ends are indicated. A.U., arbitrary units. (D) Analysis of chromatin-bound RPA32 in *LigIV*$^{-/-}$ and *LigIV*$^{-/-}$:*53BP1*$^{-/-}$ abl pre-B cells expressing either ctr, KAP-1, or CtIP shRNA. Cells were treated with imatinib for 2 days and then treated with 5 μg/ml bleocin for 24 h. RPA32 retention in the nucleus was assessed and quantified as the fraction of RPA-positive cells either treated or not treated with bleocin. Data shown were generated from *LigIV*$^{-/-}$:*DEL*^{CJ}-7 and *LigIV*$^{-/-}$:*53BP1*$^{-/-}$:*DEL*^{CJ}-5 abl pre-B cells. Similar results were obtained for *LigIV*$^{-/-}$:*DEL*^{CJ}-10 and *LigIV*$^{-/-}$:*53BP1*$^{-/-}$:*DEL*^{CJ}-6 abl pre-B cells.

down of KAP-1 leads to reduced resection of coding ends at the *Igk* locus and pMX-DEL^{CJ} in *LigIV*$^{-/-}$:*H2AX*$^{-/-}$:*DEL*^{CJ} and *LigIV*$^{-/-}$:*53BP1*$^{-/-}$:*DEL*^{CJ} abl pre-B cells (Fig. 2A to C; see also the data posted at the URL mentioned above). This was evidenced by an increase in full-length coding ends at pMX-DEL^{CJ} and *Igk* in *LigIV*$^{-/-}$:*H2AX*$^{-/-}$:*DEL*^{CJ} and *LigIV*$^{-/-}$:*53BP1*$^{-/-}$:*DEL*^{CJ} abl pre-B cells expressing a KAP-1 shRNA compared to those expressing a control shRNA (Fig. 2B and C; see also the data posted at the URL mentioned above).

In *LigIV*$^{-/-}$:*53BP1*$^{-/-}$:*DEL*^{CJ} abl pre-B cells, many pMX-DEL^{CJ} coding ends were extensively resected and thus not detected by the C4b probe (Fig. 2B). However, knockdown of KAP-1 led to diminished resection of these DNA ends, which became detectable as full-length or partially resected ends (Fig. 2B). Knockdown of CtIP using a CtIP shRNA in *LigIV*$^{-/-}$:*H2AX*$^{-/-}$:*DEL*^{CJ} and *LigIV*$^{-/-}$:*53BP1*$^{-/-}$:*DEL*^{CJ} abl pre-B cells severely limited resection at pMX-DEL^{CJ} and *Igk* (Fig. 2B and C; see also the data posted at http://pathology.wustl.edu/labs/sleckman/Tubbs_et_a_MCB_2014_Supplement.pdf). Thus, nearly all of the resection in this setting is dependent on CtIP, consistent with previous studies (11). These data suggest that KAP-1 supports CtIP-mediated resection of RAG DSBs in the absence of H2AX and 53BP1.

DNA end resection can lead to the formation of single-strand overhangs that bind the RPA complex. RPA binding to single-strand DNA can be detected by retention of the RPA32 subunit in the nucleus after DNA damage, as measured by flow cytometry (34). Treatment of *LigIV*$^{-/-}$:*53BP1*$^{-/-}$ abl pre-B cells arrested in G_1 phase with the DNA DSB-inducing agent bleocin led to a dramatic increase in RPA32 retention in the nucleus, compared to *LigIV*$^{-/-}$ abl pre-B cells (Fig. 2D). Knockdown of KAP-1 or CtIP in *LigIV*$^{-/-}$:*53BP1*$^{-/-}$ abl pre-B cells caused a significant decrease in the retention of RPA32 (Fig. 2D). Together, these data demonstrate that KAP-1 is required to promote the resection of DNA DSBs generated in G_1-phase lymphocytes that are deficient in H2AX or 53BP1.

Human KAP-1 does not promote resection of RAG DSBs in murine lymphocytes. A broad variety of human KAP-1 mutants have been generated, which could be used to define KAP-1 function during DNA end resection (36). To this end, we knocked

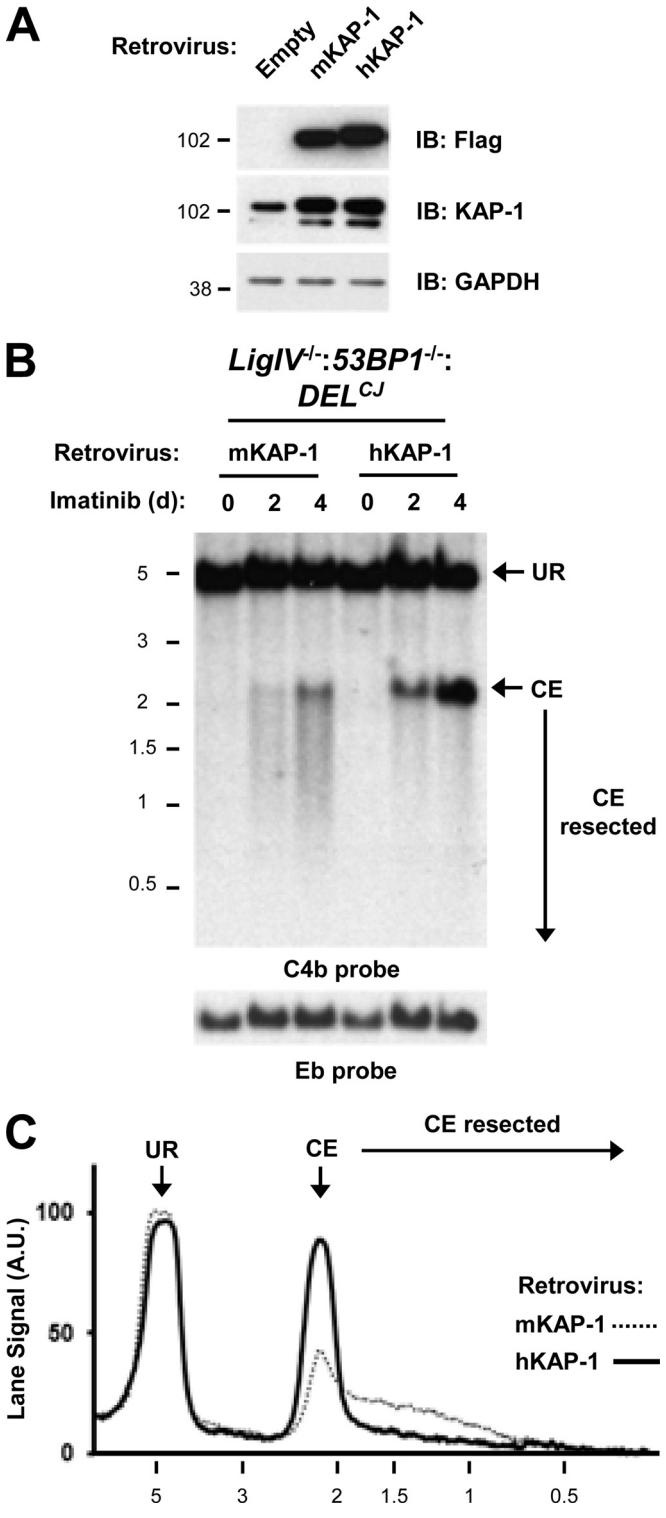

FIG 3 Expression of human KAP-1 blocks resection of RAG DSBs. (A) Immunoblot analysis of ectopic KAP-1 expression in *LigIV*$^{-/-}$:*53BP1*$^{-/-}$ abl pre-B cells expressing either an empty retrovirus (Empty) or a retrovirus encoding Flag–HA–mouse KAP-1 (mKAP-1) or Flag–HA–human KAP-1 (hKAP-1) proteins. Blots were probed with anti-Flag, anti-KAP-1, and anti-GAPDH as a loading control. (B) Southern blot analysis of pMX-DEL^{CJ} as described in the legend of Fig. 1A. *LigIV*$^{-/-}$:*53BP1*$^{-/-}$:*DEL*^{CJ} abl pre-B cells expressing a retrovirus encoding Flag-HA-tagged mKAP-1 or hKAP-1 were treated with imatinib for the indicated numbers of days. (C) Density plots comparing lane signals from *LigIV*$^{-/-}$:*53BP1*$^{-/-}$:*DEL*^{CJ} abl pre-B cells in panel B at 4 days of imatinib treatment, as described in the legend of Fig. 2C. Data shown were generated from *LigIV*$^{-/-}$:*53BP1*$^{-/-}$:*DEL*^{CJ}-6 abl pre-B cells, and similar results were obtained for *LigIV*$^{-/-}$:*53BP1*$^{-/-}$:*DEL*^{CJ}-5 abl pre-B cells.

down KAP-1 in *LigIV*$^{-/-}$:*53BP1*$^{-/-}$:*DEL*^{CJ} abl pre-B cells and expressed shRNA-resistant cDNAs encoding either mouse KAP-1 (mKAP-1) or human KAP-1 (hKAP-1). The expression levels of these two proteins are similar to that of endogenous KAP-1 (see the data posted at http://pathology.wustl.edu/labs/sleckman/Tubbs_et_a_MCB_2014_Supplement.pdf). As expected, robust resection of pMX-DEL^{CJ} coding ends was observed for *LigIV*$^{-/-}$:*53BP1*$^{-/-}$:*DEL*^{CJ} abl pre-B cells expressing mKAP-1 (see the data posted at the URL mentioned above). However, cells expressing hKAP-1 had reduced coding end resection at pMX-DEL^{CJ} (see the data posted at the URL mentioned above), which, surprisingly, suggests that hKAP-1 may be defective in mediating resection in murine cells. In addition, ectopic expression of hKAP-1 but not mKAP-1 in *LigIV*$^{-/-}$:*53BP1*$^{-/-}$:*DEL*^{CJ} abl pre-B cells resulted in a significant reduction of coding end resection at pMX-DEL^{CJ}, even without knockdown of endogenous mKAP-1 (Fig. 3). We conclude that hKAP-1 is not able to promote coding end resection in murine lymphocytes. Moreover, expression of hKAP-1 prevents endogenous mKAP-1 from functioning in DNA end resection.

DNA end resection activity localizes to an uncharacterized region of KAP-1. mKAP-1 and hKAP-1 share 93% identity, with a total of 57 amino acid differences distributed along the length of the protein (see the data posted at http://pathology.wustl.edu/labs/sleckman/Tubbs_et_a_MCB_2014_Supplement.pdf). To determine which differences compromise KAP-1 DNA end resection activity in mouse cells, we generated and analyzed a series of hybrids between mKAP-1 and hKAP-1. mKAP-1^{h1-411} has amino acids 1 to 411 replaced by the corresponding amino acids from hKAP-1. Similarly, mKAP-1$^{h412-835}$ has amino acids 412 to 835 replaced by the corresponding hKAP-1 amino acids (Fig. 4A). Thus, mKAP-1^{h1-411} is composed of the N-terminal half of hKAP-1 and the C-terminal half of mKAP-1, whereas mKAP-1$^{h412-835}$ is composed of the N-terminal half of mKAP-1 and the C-terminal half of hKAP-1.

LigIV$^{-/-}$:*53BP1*$^{-/-}$:*DEL*^{CJ} abl pre-B cells expressing mKAP-1^{h1-411} exhibit robust pMX-DEL^{CJ} coding end resection, whereas coding ends are not resected in cells expressing mKAP-1$^{h412-835}$ (Fig. 4A; see also the data posted at http://pathology.wustl.edu/labs/sleckman/Tubbs_et_a_MCB_2014_Supplement.pdf). Thus, the C-terminal half of mKAP-1 appears to be critical for promoting resection. Two additional KAP-1 hybrids that further divide this region were generated. mKAP-1$^{h412-623}$ contains the HP1-binding domain and flanking region from hKAP-1, whereas mKAP-1$^{h624-835}$ contains the C-terminal PHD, bromodomain, and flanking regions of hKAP-1. mKAP-1$^{h624-835}$, but not mKAP-1$^{h412-623}$, is able to promote pMX-DEL^{CJ} coding end resection in *LigIV*$^{-/-}$:*53BP1*$^{-/-}$:*DEL*^{CJ} abl pre-B cells (Fig. 4B; see also the data posted at the URL mentioned above). The region between amino acids 412 and 623 was further divided, generating mKAP-1$^{h412-530}$ and mKap-1$^{h531-623}$. While pMX-DEL^{CJ} coding end resection was robust in *LigIV*$^{-/-}$:*53BP1*$^{-/-}$:*DEL*^{CJ} abl pre-B cells expressing mKAP-1$^{h412-530}$, minimal resection was observed in cells expressing mKAP-1$^{h531-623}$ (Fig. 4C; see also the data posted at the URL mentioned above).

Thus, replacing amino acids 531 to 623 of mKAP-1 with the

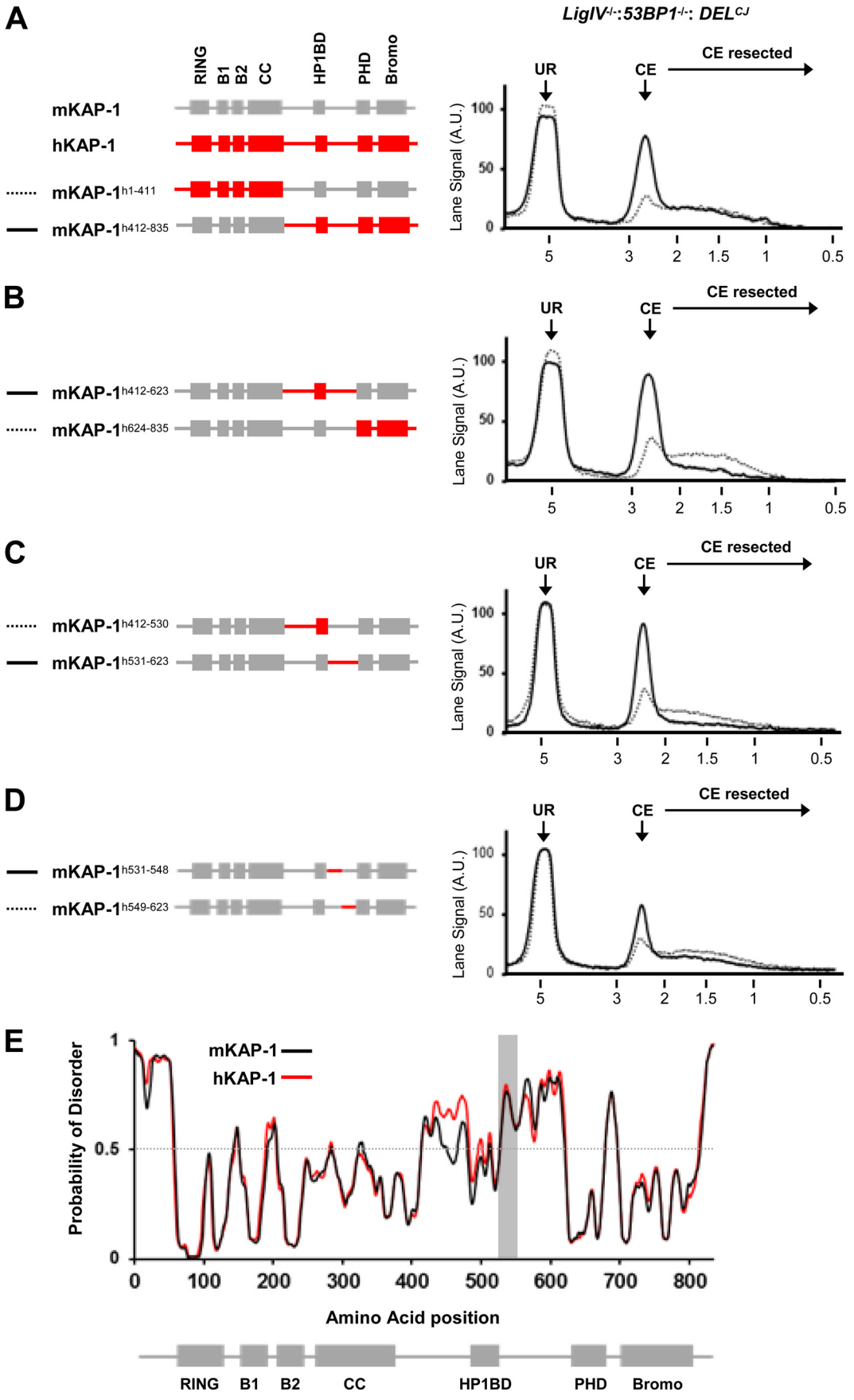

corresponding amino acids from hKAP-1 renders mKAP-1 unable to promote coding end resection in *LigIV*$^{-/-}$:*53BP1*$^{-/-}$:*DEL*^{CJ} abl pre-B cells. This region of KAP-1 does not contain known functional domains, but it is proline rich, a general feature of regions with intrinsically disordered regions (37). Indeed, analyses of mKAP-1 and hKAP-1 using the PrDOS algorithm predicts that this region would be disordered, implying that this region serves as a flexible tether between ordered domains (Fig. 4E) (33).

A single-amino-acid polymorphism defines KAP-1 function in DNA end resection. mKAP-1 and mKAP-1$^{h531-623}$ differ by 19 amino acids. A subsequent set of KAP-1 hybrid proteins showed that mKAP-1$^{h549-623}$ is able to promote coding end resection, whereas mKAP-1$^{h531-548}$ is not (Fig. 4D; see also the data posted at http://pathology.wustl.edu/labs/sleckman/Tubbs_et_a_MCB_2014_Supplement.pdf). mKAP-1$^{h531-548}$ differs from mKAP-1 by only 6 amino acids, which were each individually changed to the corresponding amino acid in hKAP-1 and expressed in *LigIV*$^{-/-}$:*53BP1*$^{-/-}$:*DEL*^{CJ} abl pre-B cells (Fig. 5A and B). All of these mKAP-1 proteins are able to promote robust coding end resection, except for mKAP-1^{P548A} (Fig. 5C; see also the data posted at the URL mentioned above), which has a single-amino-acid change at position 548 from a proline, normally present in mKAP-1, to an alanine, normally present in hKAP-1. Thus, a single-amino-acid change renders mKAP-1 unable to promote coding end resection in murine lymphocytes.

Analysis of KAP-1 sequences across species revealed that the alanine at position 548 is highly conserved in primates, whereas the proline at this position is highly conserved in most other mammals (see the data posted at http://pathology.wustl.edu/labs/sleckman/Tubbs_et_a_MCB_2014_Supplement.pdf). To confirm whether this single-amino-acid polymorphism dictates the ability of KAP-1 to function in DNA end resection in murine cells, we generated a version of hKAP-1 where the alanine at position 548 was changed to a proline (hKAP-1^{A548P}). In striking contrast to the expression of hKAP-1, *LigIV*$^{-/-}$:*53BP1*$^{-/-}$:*DEL*^{CJ} abl pre-B cells that express hKAP-1^{A548P} exhibit robust coding end resection (Fig. 5D to F). Thus, the change of alanine to proline at position 548 allows hKAP-1 to promote DNA end resection in murine cells. Together, these data demonstrate that the proline at position 548 is critical for KAP-1 activity in promoting DNA end resection.

KAP-1 promotes opening of hairpin-sealed coding ends in cells deficient in Artemis and H2AX. In the absence of H2AX or 53BP1, CtIP can efficiently open hairpin-sealed coding ends in Artemis-deficient pre-B cells (data not shown; see also the data posted at http://pathology.wustl.edu/labs/sleckman/Tubbs_et_a_MCB_2014_Supplement.pdf) (11). Artemis-deficient abl pre-B cells have hairpin-sealed coding ends that migrate at a higher molecular weight under denaturing conditions than the open coding ends in DNA ligase IV-deficient abl pre-B cells (Fig. 6A; see also the data posted at the URL mentioned above) (11). This is due to the phosphodiester bond connecting the two DNA strands of hairpin-sealed DNA ends (see also the data posted at the URL mentioned above). We expressed hKAP-1, mKAP-1, mKAP-1^{P548A}, and hKAP-1^{A548P} in *Art*$^{-/-}$:*H2AX*$^{-/-}$:*DEL*^{CJ} abl pre-B cells and assayed coding end structure by denaturing Southern blot analysis (Fig. 6B and C). These analyses revealed that coding ends are readily opened in *Art*$^{-/-}$:*H2AX*$^{-/-}$:*DEL*^{CJ} abl pre-B cells that express mKAP-1 or hKAP-1^{A548P} but not in those that express hKAP-1 or mKAP-1^{P548A} (Fig. 6B and C). Thus, in abl pre-B cells deficient in H2AX and Artemis, KAP-1 is required to promote opening of hairpin-sealed coding ends.

KAP-1 promotes resection of non-RAG DSBs in G_1-phase lymphocytes. We wished to determine whether KAP-1 influences the processing of other types of DNA ends in G_1-phase lymphocytes. To this end, we made use of a previously described pair of zinc finger endonuclease fusions, Eb:ZFN1 and Eb:ZFN2, collectively referred to as Eb:ZFN, that generate a DNA DSB at the *Tcrb* locus (30). Eb:ZFN can be expressed in abl pre-B cells under the control of a tetracycline-inducible promoter. Induction of Eb:ZFN in *LigIV*$^{-/-}$ abl pre-B cells arrested in G_1 phase with imatinib results in a DSB at the *Tcrb* locus that is not repaired, due to the deficiency in DNA ligase IV (Fig. 7A). Eb:ZFN induction in *LigIV*$^{-/-}$:*53BP1*$^{-/-}$ abl pre-B cells leads to the generation of DSBs at the *Tcrb* locus that are resected, similar to coding ends generated by RAG cleavage in these cells (Fig. 7A). Moreover, this resection is dependent on ATM, as it is significantly diminished by the addition of the ATM inhibitor KU55933 (Fig. 7A). *LigIV*$^{-/-}$:*53BP1*$^{-/-}$ abl pre-B cells that express mKAP-1^{P548A} are unable to resect DNA ends generated by Eb:ZFN (Fig. 7B). Thus, like RAG DSBs, in G_1-phase lymphocytes deficient in 53BP1, KAP-1 promotes the resection of DNA DSBs generated by a zinc finger endonuclease.

DISCUSSION

53BP1 and γ-H2AX function to protect DNA ends from nucleolytic resection initiated by CtIP in G_1-phase cells. Retention of 53BP1 at DSBs depends on γ-H2AX (24). Thus, promoting 53BP1 retention at DSBs could be the primary function of γ-H2AX in modulating DNA end processing in G_1-phase cells. However, coding ends generally exhibit greater resection in 53BP1-deficient than in H2AX-deficient cells. This could be due to the transient association of 53BP1 with DSBs in H2AX-deficient cells (24). Alternatively, in addition to retaining 53BP1 at broken DNA ends, γ-H2AX may also promote resection of DNA ends in the absence of 53BP1. The possibility that γ-H2AX promotes resection is consistent with its function in HR (38). Thus, similar to ATM, H2AX may have multiple roles in DNA end resection (11).

Here, we show that 53BP1 and H2AX protect DNA ends, at least in part, by suppressing the activity of the TRIM family protein KAP-1, which promotes the aberrant resection of DSBs in G_1-phase cells. At RAG DSBs in murine lymphocytes, proper KAP-1 activity is required for efficient opening of hairpin-sealed coding ends when cells are deficient in Artemis and H2AX, dem-

FIG 4 Effect of KAP-1 mouse-human hybrids on resection of RAG DSBs. (A to D, left) Linear diagrams of mKAP-1, hKAP-1, and human-mouse hybrids, as described in the text. mKAP-1 domains are shown in gray, while hKAP-1 domains are shown in red. All KAP-1 hybrid proteins are Flag tagged at the N terminus. (Right) Density plots comparing lane signals from Southern blot analyses of pMX-DEL^{CJ}, as described in the legend of Fig. 2C, in *LigIV*$^{-/-}$:*53BP1*$^{-/-}$:*DEL*^{CJ} abl pre-B cells expressing a retrovirus encoding the indicated KAP-1 hybrid proteins treated with imatinib for 4 days. Primary data are posted at http://pathology.wustl.edu/labs/sleckman/Tubbs_et_a_MCB_2014_Supplement.pdf. Dotted lines represent KAP-1 hybrids that function similarly to mKAP-1 to promote resection. Solid lines represent KAP-1 hybrids that function to inhibit resection. Data shown were generated from *LigIV*$^{-/-}$:*53BP1*$^{-/-}$:*DEL*^{CJ}-6 abl pre-B cells. (E) Probability of disorder, as determined by PrDOS, along the linear amino acid sequences of hKAP-1 and mKAP-1. The gray box indicates the region between amino acids 531 and 548, which is predicted to be disordered.

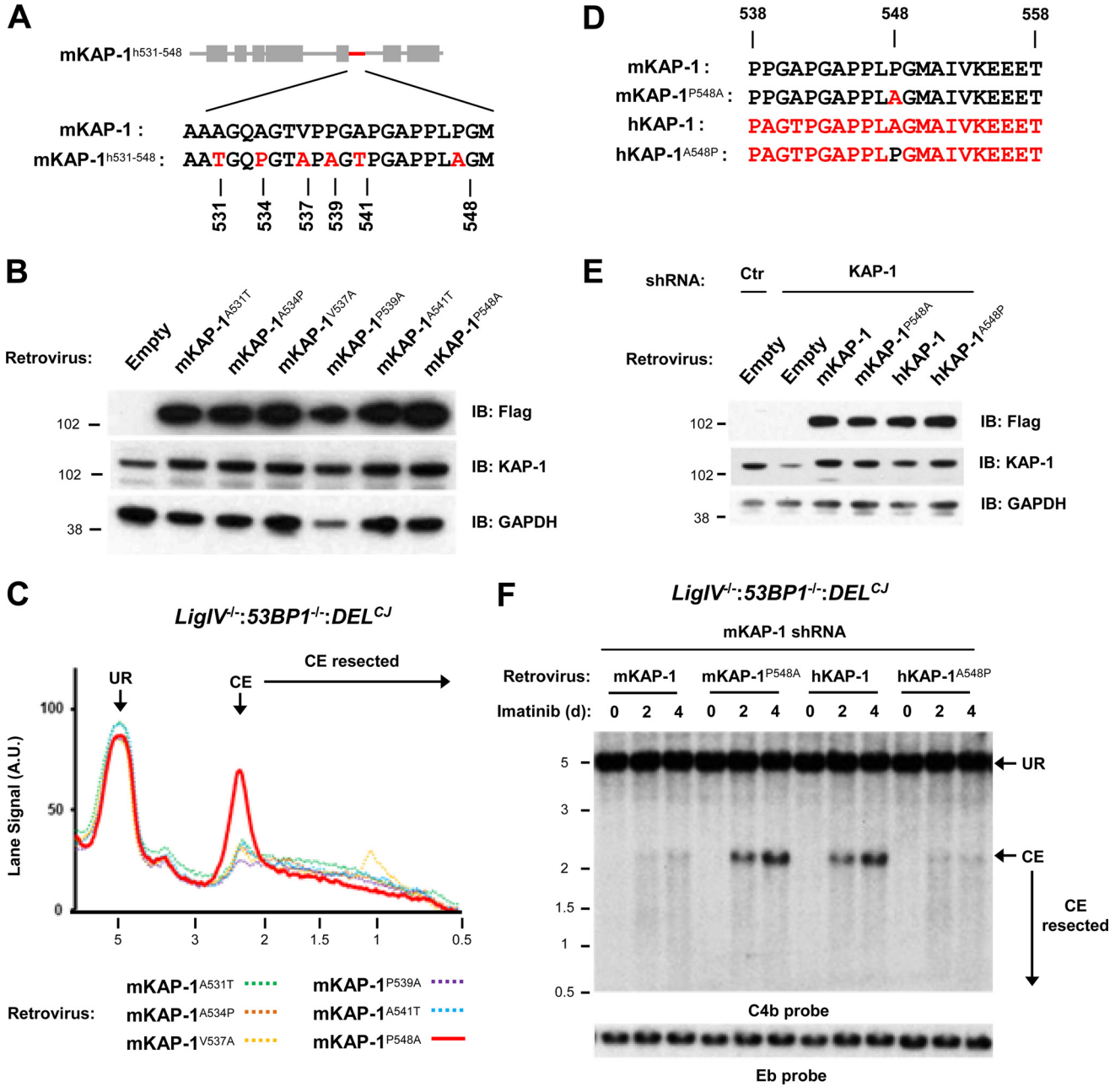

FIG 5 A single-amino-acid change at position 548 determines KAP-1 functionality during resection of RAG DSBs. (A) Comparison of amino acid discrepancies between mKAP-1 and mKAP-1$^{h531–548}$. Human-specific residues are highlighted in red. (B) Immunoblot analysis of *LigIV*$^{-/-}$:*53BP1*$^{-/-}$:*DEL*^{CJ} abl pre-B cells expressing either an empty retrovirus (Empty) or a retrovirus encoding the indicated mKAP-1 point mutants. All mutants are Flag tagged at the N terminus. (C) Density plots comparing lane signals from Southern blot analyses of pMX-DEL^{CJ}, as described in the legend of Fig. 2C, in *LigIV*$^{-/-}$:*53BP1*$^{-/-}$:*DEL*^{CJ}-6 abl pre-B cells expressing a retrovirus encoding the indicated mKAP-1 point mutants treated with imatinib for 4 days. Primary data are posted at http://pathology.wustl.edu/labs/sleckman/Tubbs_et_a_MCB_2014_Supplement.pdf. (D) Amino acid sequence surrounding position 548 in mKAP-1, mKAP-1^{P548A}, hKAP-1, and hKAP-1^{A548P}. Human-specific residues are highlighted in red. (E) Immunoblot analysis of *LigIV*$^{-/-}$:*53BP1*$^{-/-}$:*DEL*^{CJ} abl pre-B cells expressing either a ctr shRNA or KAP-1 shRNA in addition to an empty retrovirus or a retrovirus encoding Flag-HA-tagged mKAP-1, mKAP-1^{P548A}, hKAP-1, or hKAP-1^{A548P}. (F) Southern blot analysis of pMX-DEL^{CJ}, as described in the legend of Fig. 1A. *LigIV*$^{-/-}$:*53BP1*$^{-/-}$:*DEL*^{CJ} abl pre-B cells expressing KAP-1 shRNA in addition to a retrovirus encoding mKAP-1, mKAP-1^{P548A}, hKAP-1, or hKAP-1^{A548P} were treated with imatinib for the indicated numbers of days. Data shown were generated from *LigIV*$^{-/-}$:*53BP1*$^{-/-}$:*DEL*^{CJ}-5 abl pre-B cells, and similar results were obtained for *LigIV*$^{-/-}$:*53BP1*$^{-/-}$:*DEL*^{CJ}-6 abl pre-B cells.

onstrating that KAP-1 functions at the earliest step of the resection process. In addition to RAG DSBs, mouse KAP-1 promotes the resection of DNA ends generated by a ZFN and by DNA-damaging agents, such as bleocin. Based on our data, CtIP and KAP-1 may be part of the same pathway that generates resection at DNA DSBs in G_1-phase cells. It is possible that these two proteins normally interact at DNA DSBs to promote resection, either directly or in a sequential manner, where KAP-1 is required for optimal

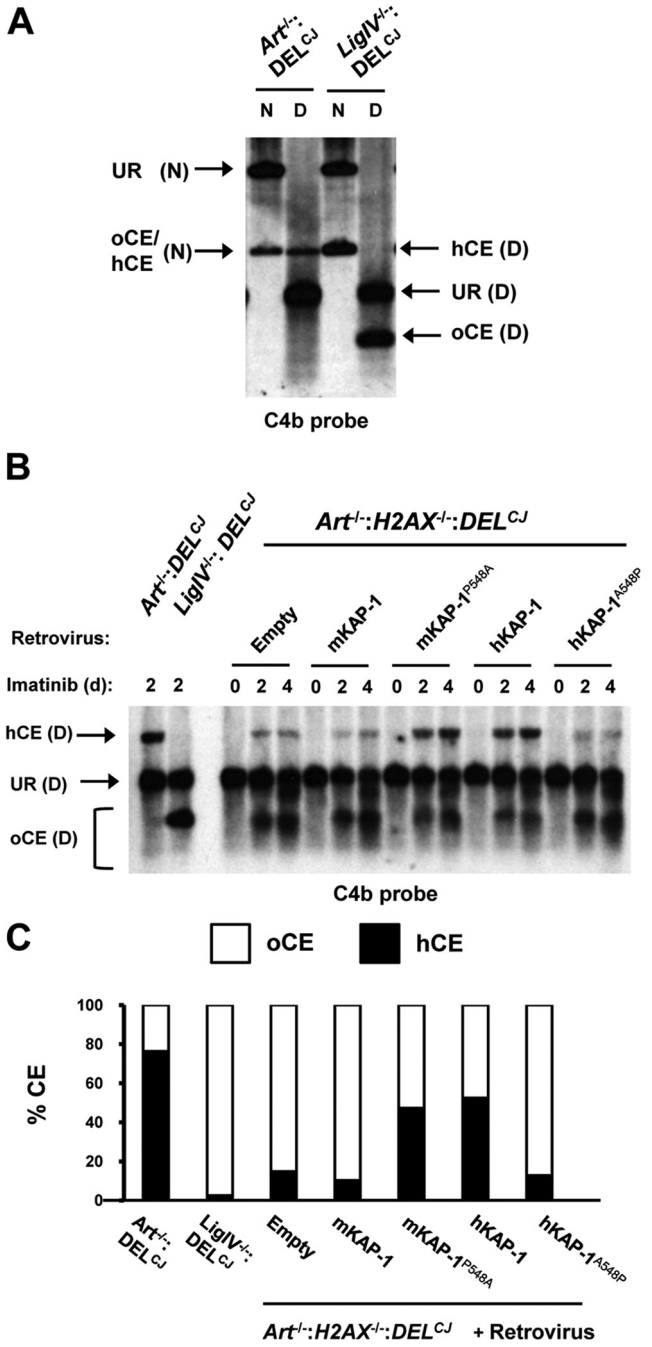

FIG 6 KAP-1 is required for opening of hairpin-sealed coding ends in the absence of Artemis. (A) Denaturing Southern blot analysis of pMX-DEL^{CJ}. EcoRV-digested genomic DNA from *Art*$^{-/-}$:*DEL*^{CJ} and *LigIV*$^{-/-}$:*DEL*^{CJ} abl pre-B cells treated with imatinib for 2 days were either denatured (D) or left nondenatured (N). Nondenatured (N) and denatured (D) bands distinguishing unrearranged pMX-DEL^{CJ} (UR), hairpin-sealed coding ends (hCE), and open coding ends (oCE) are labeled. (B) Denaturing Southern blot analysis of pMX-DEL^{CJ} as described above for panel A. *Art*$^{-/-}$:*DEL*^{CJ}, *LigIV*$^{-/-}$:*DEL*^{CJ}, and *Art*$^{-/-}$:*H2AX*$^{-/-}$:*DEL*^{CJ} abl pre-B cells expressing either an empty retrovirus or a retrovirus encoding Flag-HA-tagged mKAP-1, mKAP-1^{P548A}, hKAP-1, or hKAP-1^{A548P} were analyzed after imatinib treatment for the indicated numbers of days. (C) Bar graph showing the percentages of pMX-DEL^{CJ} coding ends that are either hairpin sealed or open, as quantitated from denaturing Southern blot lanes at 2 days of imatinib treatment in panel B. Data shown were generated from *Art*$^{-/-}$:*H2AX*$^{-/-}$:*DEL*^{CJ}-95 abl pre-B cells, and similar results were obtained with *Art*$^{-/-}$:*H2AX*$^{-/-}$:*DEL*^{CJ}-124 abl pre-B cells.

CtIP activity. Thus, KAP-1 is a component of the DNA end resection machinery that can function in murine G_1-phase lymphocytes, and its activity must be regulated by γ-H2AX and 53BP1 to prevent aberrant DNA end processing that could lead to the formation of chromosomal translocations and deletions.

In heterochromatin, repair of DSBs requires phosphorylation of KAP-1 at serine 824 by ATM (14, 15, 21), which is dispensable for DSB repair in euchromatin (15, 21). We have found a new role for mouse KAP-1 that is not limited to heterochromatin, as murine KAP-1 promotes the resection of unprotected RAG DSBs, which are generated at transcribed, accessible loci (39). We show that the KAP-1 function in promoting DNA end resection in 53BP1-deficient cells depends on a proline-rich region that is predicted to be intrinsically disordered. In this region, the integrity of a single proline residue at position 548 is critical, and changing this residue to an alanine, found in human KAP-1, compromises mouse KAP-1 resection activity. Moreover, converting the alanine to a proline at this position in human KAP-1 enables resection activity in murine cells.

In the absence of 53BP1, G_1-phase lymphocytes expressing mKAP-1^{P548A} are unable to efficiently resect DSBs generated by RAG or a ZFN, even when wild-type mouse KAP-1 is expressed at normal levels. KAP-1 exists as a stable homotrimer in the cell, raising the possibility that the incorporation of one or more mKAP-1^{P548A} proteins into this trimer disrupts KAP-1 activity in a dominant manner. Knockdown of murine KAP-1 leads to a defect in resection that is less severe than that observed with ectopic expression of mKAP-1^{P548A}. It is possible that the residual mouse KAP-1 homotrimers remaining after knockdown are sufficient to promote DNA end resection albeit at a reduced level.

The proline at position 548 in mouse KAP-1 is part of a PxxP motif, which could serve as a ligand to bind proteins with an SH3 domain (40). Thus, the conversion of proline to alanine could disrupt the mouse KAP-1 association with a protein containing an SH3 domain that is required for DNA end resection. Disordered domains, especially those that encompass proline-rich regions, can also mediate protein-protein interactions through proline-rich motifs. The interactions through these motifs might be disrupted by the alanine substitution (41, 42). Finally, this substitution could influence the ability of distinct mouse KAP-1 domains to cooperatively function with each other in the setting of a single mouse KAP-1 molecule or homotrimer.

The inability of human KAP-1, a TRIM family protein member, to promote resection of broken DNA ends in murine cells was surprising, as was the modulation of this activity by a single-amino-acid difference at position 548. The proline residue at position 548 is highly conserved across all mammals except primates, where there has been a conversion to alanine. In this regard, integrating TRIM proteins as components of generally conserved DNA damage responses may pose unique evolutionary challenges, given the diverse activities that TRIM proteins mediate. Some of these activities, such as responses to pathogens, necessitate significant TRIM protein sequence divergence over short evolutionary distances. For example, TRIM5α binds to the HIV capsid protein, preventing virus entry into the cytoplasm (18). Whereas human and rhesus monkey TRIM5α proteins have this activity, mouse TRIM5α does not (18).

Human KAP-1 (TRIM28) has also recently been shown to have important functions in preventing HIV integration into the genome (43). Thus, primate KAP-1 could have acquired evolution-

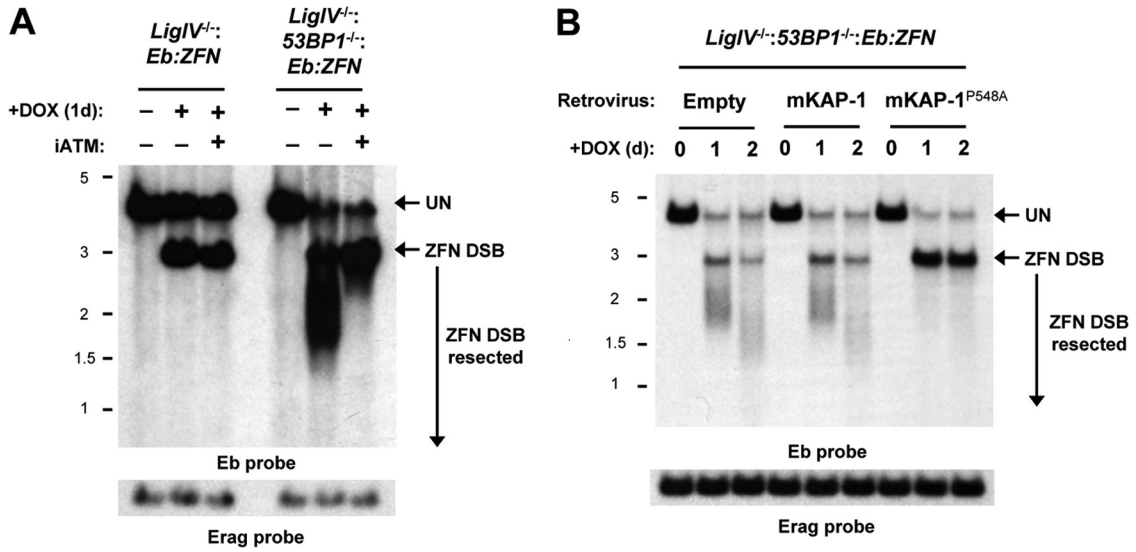

FIG 7 KAP-1 promotes resection of non-RAG DSBs in G_1-phase lymphocytes. (A) Southern blot analysis of the endogenous *Tcrb* locus. *LigIV*$^{-/-}$:Eb:ZFN and *LigIV*$^{-/-}$:*53BP1*$^{-/-}$:*Eb*:*ZFN* abl pre-B cells were treated with imatinib for 1 day and then treated with doxycycline for 1 day in presence or absence of the ATM inhibitor (ATMi) KU55933. Genomic DNA was digested with HindIII, and blots were hybridized with an Eb probe. An Erag probe was used as a DNA loading control. Uncut *Tcrb* (UN) and unrepaired ZFN DSBs are indicated, as are as resected ZFN DSBs. (B) Southern blot analysis of the endogenous *Tcrb* locus, as described above for panel A. *LigIV*$^{-/-}$:*53BP1*$^{-/-}$:Eb:ZFN abl pre-B cells were infected with either an empty retrovirus or a retrovirus expressing Flag–HA–mKAP-1 or Flag–HA–mKAP-1^{P548A}. Cells were pretreated with imatinib for 1 day, and doxycycline was then added for the indicated numbers of days.

arily recent changes that have been selected for this or other activities unique to primate cells. While beneficial for pathogen responses, these changes may be detrimental to other primate KAP-1 functions, such as those involved in DNA DSB repair. It is possible that primates do not rely on this KAP-1 activity in DSB repair. However, it is also possible that in primates, this activity is carried out by other TRIM family paralogues. Alternatively, primates may have evolved compensatory changes in DSB repair proteins that allow these proteins to function with primate KAP-1 to promote resection. Indeed, recent studies have suggested that DNA repair genes have undergone adaptive evolution, particularly at regions critical for protein-protein interactions (44).

ACKNOWLEDGMENTS

We thank Tanya Paull, Jeff Bednarski, and Bo-Ruei Chen for critical review of the manuscript.

This work was supported by National Institutes of Health grants CA136470 (B.P.S.), AI074953 (B.P.S.), AI47829 (B.P.S.), and AI49934 (M.S.K.).

REFERENCES

1. **Lieber MR.** 2010. The mechanism of double-strand DNA break repair by the nonhomologous DNA end-joining pathway. Annu. Rev. Biochem. **79:**181–211. http://dx.doi.org/10.1146/annurev.biochem.052308.093131.
2. **Ciccia A, Elledge SJ.** 2010. The DNA damage response: making it safe to play with knives. Mol. Cell **40:**179–204. http://dx.doi.org/10.1016/j.molcel.2010.09.019.
3. **Symington LS, Gautier J.** 2011. Double-strand break end resection and repair pathway choice. Annu. Rev. Genet. **45:**247–271. http://dx.doi.org/10.1146/annurev-genet-110410-132435.
4. **Huertas P.** 2010. DNA resection in eukaryotes: deciding how to fix the break. Nat. Struct. Mol. Biol. **17:**11–16. http://dx.doi.org/10.1038/nsmb.1710.
5. **Tonegawa S.** 1983. Somatic generation of antibody diversity. Nature **302:**575–581. http://dx.doi.org/10.1038/302575a0.
6. **Fugmann SD, Lee AI, Shockett PE, Villey IJ, Schatz DG.** 2000. The RAG proteins and V(D)J recombination: complexes, ends, and transposition. Annu. Rev. Immunol. **18:**495–527. http://dx.doi.org/10.1146/annurev.immunol.18.1.495.
7. **Helmink BA, Sleckman BP.** 2012. The response to and repair of RAG-mediated DNA double-strand breaks. Annu. Rev. Immunol. **30:**175–202. http://dx.doi.org/10.1146/annurev-immunol-030409-101320.
8. **Rooney S, Chaudhuri J, Alt FW.** 2004. The role of the non-homologous end-joining pathway in lymphocyte development. Immunol. Rev. **200:**115–131. http://dx.doi.org/10.1111/j.0105-2896.2004.00165.x.
9. **Zha S, Guo C, Boboila C, Oksenych V, Cheng HL, Zhang Y, Wesemann DR, Yuen G, Patel H, Goff PH, Dubois RL, Alt FW.** 2011. ATM damage response and XLF repair factor are functionally redundant in joining DNA breaks. Nature **469:**250–254. http://dx.doi.org/10.1038/nature09604.
10. **Li G, Alt FW, Cheng HL, Brush JW, Goff PH, Murphy MM, Franco S, Zhang Y, Zha S.** 2008. Lymphocyte-specific compensation for XLF/cernunnos end-joining functions in V(D)J recombination. Mol. Cell **31:**631–640. http://dx.doi.org/10.1016/j.molcel.2008.07.017.
11. **Helmink BA, Tubbs AT, Dorsett Y, Bednarski JJ, Walker LM, Feng Z, Sharma GG, McKinnon PJ, Zhang J, Bassing CH, Sleckman BP.** 2011. H2AX prevents CtIP-mediated DNA end resection and aberrant repair in G_1-phase lymphocytes. Nature **469:**245–249. http://dx.doi.org/10.1038/nature09585.
12. **Desiderio S, Lin WC, Li Z.** 1996. The cell cycle and V(D)J recombination. Curr. Top. Microbiol. Immunol. **217:**45–59.
13. **Savic V, Yin B, Maas NL, Bredemeyer AL, Carpenter AC, Helmink BA, Yang-Iott KS, Sleckman BP, Bassing CH.** 2009. Formation of dynamic gamma-H2AX domains along broken DNA strands is distinctly regulated by ATM and MDC1 and dependent upon H2AX densities in chromatin. Mol. Cell **34:**298–310. http://dx.doi.org/10.1016/j.molcel.2009.04.012.
14. **Ziv Y, Bielopolski D, Galanty Y, Lukas C, Taya Y, Schultz DC, Lukas J, Bekker-Jensen S, Bartek J, Shiloh Y.** 2006. Chromatin relaxation in response to DNA double-strand breaks is modulated by a novel ATM- and KAP-1 dependent pathway. Nat. Cell Biol. **8:**870–876. http://dx.doi.org/10.1038/ncb1446.
15. **Goodarzi AA, Jeggo P, Lobrich M.** 2010. The influence of heterochromatin on DNA double strand break repair: getting the strong, silent type to relax. DNA Repair (Amst.) **9:**1273–1282. http://dx.doi.org/10.1016/j.dnarep.2010.09.013.
16. **Iyengar S, Farnham PJ.** 2011. KAP1 protein: an enigmatic master regulator of the genome. J. Biol. Chem. **286:**26267–26276. http://dx.doi.org/10.1074/jbc.R111.252569.

17. **Hatakeyama S.** 2011. TRIM proteins and cancer. Nat. Rev. Cancer **11:** 792–804. http://dx.doi.org/10.1038/nrc3139.
18. **Ozato K, Shin DM, Chang TH, Morse HC, III.** 2008. TRIM family proteins and their emerging roles in innate immunity. Nat. Rev. Immunol. **8:**849–860. http://dx.doi.org/10.1038/nri2413.
19. **Nisole S, Stoye JP, Saib A.** 2005. TRIM family proteins: retroviral restriction and antiviral defence. Nat. Rev. Microbiol. **3:**799–808. http://dx.doi.org/10.1038/nrmicro1248.
20. **Han K, Lou DI, Sawyer SL.** 2011. Identification of a genomic reservoir for new TRIM genes in primate genomes. PLoS Genet. **7:**e1002388. http://dx.doi.org/10.1371/journal.pgen.1002388.
21. **Goodarzi AA, Noon AT, Deckbar D, Ziv Y, Shiloh Y, Lobrich M, Jeggo PA.** 2008. ATM signaling facilitates repair of DNA double-strand breaks associated with heterochromatin. Mol. Cell **31:**167–177. http://dx.doi.org/10.1016/j.molcel.2008.05.017.
22. **Goodarzi AA, Kurka T, Jeggo PA.** 2011. KAP-1 phosphorylation regulates CHD3 nucleosome remodeling during the DNA double-strand break response. Nat. Struct. Mol. Biol. **18:**831–839. http://dx.doi.org/10.1038/nsmb.2077.
23. **Noon AT, Shibata A, Rief N, Lobrich M, Stewart GS, Jeggo PA, Goodarzi AA.** 2010. 53BP1-dependent robust localized KAP-1 phosphorylation is essential for heterochromatic DNA double-strand break repair. Nat. Cell Biol. **12:**177–184. http://dx.doi.org/10.1038/ncb2017.
24. **Celeste A, Fernandez-Capetillo O, Kruhlak MJ, Pilch DR, Staudt DW, Lee A, Bonner RF, Bonner WM, Nussenzweig A.** 2003. Histone H2AX phosphorylation is dispensable for the initial recognition of DNA breaks. Nat. Cell Biol. **5:**675–679. http://dx.doi.org/10.1038/ncb1004.
25. **Difilippantonio S, Gapud E, Wong N, Huang CY, Mahowald G, Chen HT, Kruhlak MJ, Callen E, Livak F, Nussenzweig MC, Sleckman BP, Nussenzweig A.** 2008. 53BP1 facilitates long-range DNA end-joining during V(D)J recombination. Nature **456:**529–533. http://dx.doi.org/10.1038/nature07476.
26. **Bunting SF, Callen E, Wong N, Chen HT, Polato F, Gunn A, Bothmer A, Feldhahn N, Fernandez-Capetillo O, Cao L, Xu X, Deng CX, Finkel T, Nussenzweig M, Stark JM, Nussenzweig A.** 2010. 53BP1 inhibits homologous recombination in Brca1-deficient cells by blocking resection of DNA breaks. Cell **141:**243–254. http://dx.doi.org/10.1016/j.cell.2010.03.012.
27. **Bothmer A, Robbiani DF, Feldhahn N, Gazumyan A, Nussenzweig A, Nussenzweig MC.** 2010. 53BP1 regulates DNA resection and the choice between classical and alternative end joining during class switch recombination. J. Exp. Med. **207:**855–865. http://dx.doi.org/10.1084/jem.20100244.
28. **Zimmermann M, Lottersberger F, Buonomo SB, Sfeir A, de Lange T.** 2013. 53BP1 regulates DSB repair using Rif1 to control 5′ end resection. Science **339:**700–704. http://dx.doi.org/10.1126/science.1231573.
29. **Bredemeyer AL, Sharma GG, Huang CY, Helmink BA, Walker LM, Khor KC, Nuskey B, Sullivan KE, Pandita TK, Bassing CH, Sleckman BP.** 2006. ATM stabilizes DNA double-strand-break complexes during V(D)J recombination. Nature **442:**466–470. http://dx.doi.org/10.1038/nature04866.
30. **Lee BS, Gapud EJ, Zhang S, Dorsett Y, Bredemeyer A, George R, Callen E, Daniel JA, Osipovich O, Oltz EM, Bassing CH, Nussenzweig A, Lees-Miller S, Hammel M, Chen BP, Sleckman BP.** 2013. Functional intersection of ATM and DNA-dependent protein kinase catalytic subunit in coding end joining during V(D)J recombination. Mol. Cell. Biol. **33:** 3568–3579. http://dx.doi.org/10.1128/MCB.00308-13.
31. **Chan EA, Teng G, Corbett E, Choudhury KR, Bassing CH, Schatz DG, Krangel MS.** 2013. Peripheral subnuclear positioning suppresses Tcrb recombination and segregates Tcrb alleles from RAG2. Proc. Natl. Acad. Sci. U. S. A. **110:**E4628–E4637. http://dx.doi.org/10.1073/pnas.1310846110.
32. **Lee DH, Goodarzi AA, Adelmant GO, Pan Y, Jeggo PA, Marto JA, Chowdhury D.** 2012. Phosphoproteomic analysis reveals that PP4 dephosphorylates KAP-1 impacting the DNA damage response. EMBO J. **31:**2403–2415. http://dx.doi.org/10.1038/emboj.2012.86.
33. **Ishida T, Kinoshita K.** 2007. PrDOS: prediction of disordered protein regions from amino acid sequence. Nucleic Acids Res. **35:**W460–W464. http://dx.doi.org/10.1093/nar/gkm363.
34. **Forment JV, Walker RV, Jackson SP.** 2012. A high-throughput, flow cytometry-based method to quantify DNA-end resection in mammalian cells. Cytometry A **81:**922–928. http://dx.doi.org/10.1002/cyto.a.22155.
35. **Bredemeyer AL, Helmink BA, Innes CL, Calderon B, McGinnis LM, Mahowald GK, Gapud EJ, Walker LM, Collins JB, Weaver BK, Mandik-Nayak L, Schreiber RD, Allen PM, May MJ, Paules RS, Bassing CH, Sleckman BP.** 2008. DNA double-strand breaks activate a multifunctional genetic program in developing lymphocytes. Nature **456:**819–823. http://dx.doi.org/10.1038/nature07392.
36. **Iyengar S, Ivanov AV, Jin VX, Rauscher FJ, III, Farnham PJ.** 2011. Functional analysis of KAP1 genomic recruitment. Mol. Cell. Biol. **31:** 1833–1847. http://dx.doi.org/10.1128/MCB.01331-10.
37. **Cheng S, Cetinkaya M, Grater F.** 2010. How sequence determines elasticity of disordered proteins. Biophys. J. **99:**3863–3869. http://dx.doi.org/10.1016/j.bpj.2010.10.011.
38. **Xie A, Puget N, Shim I, Odate S, Jarzyna I, Bassing CH, Alt FW, Scully R.** 2004. Control of sister chromatid recombination by histone H2AX. Mol. Cell **16:**1017–1025. http://dx.doi.org/10.1016/j.molcel.2004.12.007.
39. **Bassing CH, Swat W, Alt FW.** 2002. The mechanism and regulation of chromosomal V(D)J recombination. Cell **109**(Suppl)**:**S45–S55. http://dx.doi.org/10.1016/S0092-8674(02)00675-X.
40. **Mayer BJ.** 2001. SH3 domains: complexity in moderation. J. Cell Sci. **114:**1253–1263. http://jcs.biologists.org/content/114/7/1253.long.
41. **Das RK, Mittal A, Pappu RV.** 2013. How is functional specificity achieved through disordered regions of proteins? Bioessays **35:**17–22. http://dx.doi.org/10.1002/bies.201200115.
42. **Strehlow KG, Robertson AD, Baldwin RL.** 1991. Proline for alanine substitutions in the C-peptide helix of ribonuclease A. Biochemistry **30:** 5810–5814. http://dx.doi.org/10.1021/bi00237a026.
43. **Allouch A, Di Primio C, Alpi E, Lusic M, Arosio D, Giacca M, Cereseto A.** 2011. The TRIM family protein KAP1 inhibits HIV-1 integration. Cell Host Microbe **9:**484–495. http://dx.doi.org/10.1016/j.chom.2011.05.004.
44. **Demogines A, East AM, Lee JH, Grossman SR, Sabeti PC, Paull TT, Sawyer SL.** 2010. Ancient and recent adaptive evolution of primate nonhomologous end joining genes. PLoS Genet. **6:**e1001169. http://dx.doi.org/10.1371/journal.pgen.1001169.